Chinese Chemical Letters 34 (2023) 108073

Contents lists available at ScienceDirect

Chinese Chemical Letters

journal homepage: www.elsevier.com/locate/cclet

(+)/(−)-Yanhusuosines A and B, two dimeric benzylisoquinoline-protoberberine alkaloid *atropo*-enantiomers featuring polycyclic skeletons from *Corydalis yanhusuo*

Guiyang Xia[a], Biaobing Xiao[b], Lingyan Wang[a], Huan Xia[a], Yuzhuo Wu[a], Yanan Wang[b], Hongcai Shang[a], Sheng Lin[a,*]

[a] *Key Laboratory of Chinese Internal Medicine of Ministry of Education and Beijing, Dongzhimen Hospital, Beijing University of Chinese Medicine, Beijing 100700, China*

[b] *State Key Laboratory of Bioactive Substance and Function of Natural Medicines, Institute of Materia Medica, Chinese Academy of Medical Sciences and Peking Union Medical College, Beijing 100050, China*

ARTICLE INFO

Article history:
Received 12 September 2022
Revised 18 November 2022
Accepted 12 December 2022
Available online 11 January 2023

Keywords:
(+)/(−)-Yanhusuosine A
(+)/(−)-Yanhusuosine B
Bisbenzylisoquinoline alkaloids
Atropo-enantiomeric homodimers
Anti-inflammatory
Corydalis yanhusuo

ABSTRACT

(+)/(−)-Yanhusuosines A (**1**) and B (**2**), two pairs of trace benzylisoquinoline-protoberberine *atropo*-enantiomeric homodimers featuring an unprecedented 6/7/6/6/6/6 hexacyclic skeleton, were isolated from the tubers of *Corydalis yanhusuo*. The structures of (+)/(−)-**1** and (+)/(−)-**2** were elucidated using spectroscopic and quantum-chemical calculation approaches. (+)/(−)-Yanhusuosines A (**1**) and B (**2**) represent a new class of alkaloid dimers biogenetically constructed by a molecule of benzylisoquinoline with a unit of protoberberine *via* an intermolecular [4 + 3] cycloaddition. Their plausible biosynthetic pathways are discussed, and compound **2** exerted moderate inhibitory activity of NO formation in LPS induced RAW264.7 macrophages.

The bisbenzylisoquinoline alkaloids (BBIAs) are a class of special natural products that biogenetically assembled from two monomeric benzylisoquinoline alkaloids (BIAs) *via* one or two C−O−C or C−C bond connections [1–5]. During the past two decades, approximately seventy BBIAs have been characterized from the plants of Berberidaceae, Menispermaceae, and Ranunculaceae family, in particular, some of which have been found to exhibit intriguing new bioactivities [5–7]. For example, tetrandrine, a natural BBIA, is well-known to reverse multidrug resistance and inhibit Ebola virus [8]. Recently, another BBIA, cepharanthine, was reported to display remarkable inhibition against severe acute respiratory syndrome coronavirus 2 (SARS-CoV-2) [9].

The dried *Corydalis yanhusuo* W.T. Wang (Papaveraceae) tuber, a famous herbal medicine used in Asian countries, such as China, Japan, and Korean, has long been used for treating menstrual, spastic, and abdominal pain, duodenal and gastriculcers, dysmenorrhea, rheumatism, myocardial ischemia, and cardiac arrhythmias [10–13]. Among the reported compounds in this plant, BIAs are considered as the important active components of *C. yanhusuo* [14,15]. However, dimeric BIAs have rarely been reported in the Papaveraceae plants [16], especially the C−C bond linkage of two units of BIAs. Early on, two unique C−C coupled type of BBIAs with inhibitory activity against PD-1/PD-L1 interaction and anti-inflammatory activity have been identified from *C. yanhusuo* by our group [17,18]. Commonly, dimeric quaternary ammonium alkaloids usually demonstrated an intense double-charged molecular ion in the ESIMS spectrum [17–22]. During the HPLC-MS guided isolation process, a cluster of double-charged molecular ions present in the TIC data for a fraction draw our attention (Fig. S1 in Supporting information), which motivated us to target isolation of two trace benzylisoquinoline-protoberberine *atropo*-enantiomeric homodimers featuring unprecedented 6/7/6/6/6/6 hexacyclic skeleton, (+)/(−)-yanhusuosines A (**1**) and B (**2**) (Fig. 1). It is noticeable that compounds **1** and **2** represent a new class of alkaloid dimers biogenetically constructed by a benzylisoquinoline moiety coupled with a protoberberine unit *via* a [4 + 3] cycloaddition. Presented herein are the separation, structural elucidation, plausible biosynthetic pathways discussion, and biological evaluation of (+)/(−)-yanhusuosines A (**1**) and B (**2**).

Yanhusuosine A (**1**), red and amorphous powder, possessed a molecular formula of $C_{41}H_{36}N_2O_8$ based on HRESIMS data for the double-charged molecular ion at *m/z* 342.1230 (calcd. for

* Corresponding author.
E-mail address: lsznn@bucm.edu.cn (S. Lin).

https://doi.org/10.1016/j.cclet.2022.108073
1001-8417/

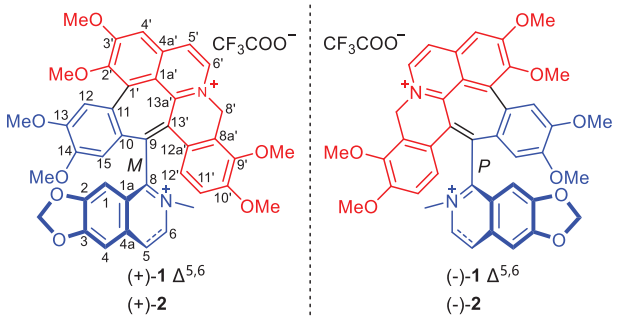

Fig. 1. Chemical structures of compounds **1** and **2**.

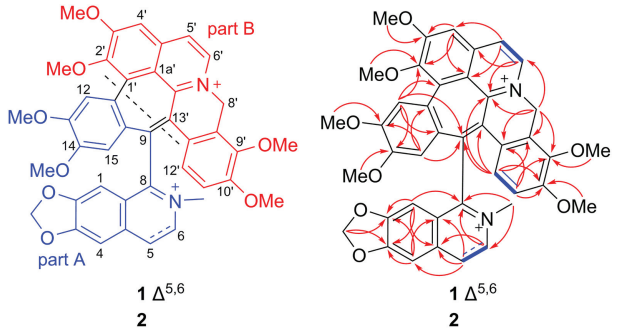

Fig. 2. Substructures (left) and selected ^{1}H-^{1}H COSY (blue thick lines) and HMBC (red arrows, from ^{1}H to ^{13}C) correlations (right) for **1** and **2**.

$C_{41}H_{36}N_2O_8$, 342.1230), in concurrence with 26 degrees of unsaturation. Its IR absorption bands at 1675, 1469, and 1446 cm^{-1} suggested the presence of C=N and aromatic functionalities. The ^{1}H NMR spectrum of yanhusuosine A (**1**) evidenced five aromatic singlets [δ_H 8.26, 7.89, 7.82, 7.60, 6.29 (each 1H, s)], three pairs of AX coupling type aromatic and/or olefinic protons [δ_H 6.98, 6.60 (each 1H, d, J = 9.0 Hz); δ_H 8.49, 8.40 (each 1H, d, J = 6.6 Hz); δ_H 8.84, 8.42 (each 1H, d, J = 6.6 Hz)], an isolated nitrogen- or oxygen-bearing methylene [δ_H 6.57, 5.88 (each 1H, d, J = 13.8 Hz)], and seven OMe and/or *N*-Me signals [δ_H 4.14, 4.08, 4.06, 3.86, 3.86, 3.67, 2.75 (each 3H, s)] (Table 1). Strikingly, two proton singlets at δ_H 6.42 and 6.49 initially assumed to be two aromatic protons, were eventually reassigned as a methylenedioxy group by the HSQC and HMBC experiments (Fig. 2). In addition to the above protonated carbons, the ^{13}C NMR coupled with the HSQC data revealed the presence of sixteen nonprotonated carbons with chemical shifts >100 ppm, implying that **1** was a highly aromatized alkaloid with complex conjugated system. This observation also matched well with the three absorption bands at 320, 420, and 500 nm in the UV spectrum.

The framework of yanhusuosine A (**1**) was constructed by interpretation of its 2D NMR spectra. The three AX coupling patterns were consistent with the COSY correlations shown in Fig. 2. A 9,11-disubsubsituted BIA moiety, part **A**, initially deduced by comparing NMR data with those of the biosynthetic analogues of BIAs from this plant [10,18], was affirmed on the basis of COSY correlations between H-5/H-6 plus HMBC and NOESY correlations summarized in Figs. 2 and 3. Similarly, the diagnostic signals attributed to protoberberine alkaloids, such as the isolated coupling of H_2-8′ [δ_H 6.57, 5.88 (each 1H, d, J = 13.8 Hz) and AX coupling patterns of H-5′/H-6′ and H-11′/H-12′ were observed. In addition, the HMBC correlations that from H-4′ to C-5′, C-2′, C-3′, and C-1a', from H-6′ to C-4a', C-13a', and C-8′, from H_2-8′ to C-6′, C-13a', C-12a', and C-9′, and from H-12′ to C-13′, C-8a', and C-10′, and C-10′ (Fig. 2) completed part **B** to be a 1′,13′-disubstitued protoberberine moiety.

Table 1
NMR spectroscopic data for **1** and **2**.

Position	**1**		**2**	
	δ_H (J in Hz) [a]	δ_C [b]	δ_H (J in Hz) [a]	δ_C [b]
1	7.60, s	103.4	7.45, s	110.8
1a		127.9		121.3
2		152.9		148.1
3		156.0		155.1
4	7.82, s	103.2	7.26, s	108.8
4a		137.7		136.5
5	8.40, d (6.6)	124.4	3.07, m	24.6
			3.50, m	
6	8.49, d (6.6)	137.0	3.76, m	52.7
			4.15, m	
8		152.3		170.5
9		132.2		131.9
10		123.8		122.4
11		122.4		122.1
12	8.26, s	109.6	8.34, s	110.0
13		149.9		148.9
14		148.5		150.5
15	6.29, s	110.0	6.90, s	110.1
-OCH_2O-	6.42, s	104.6	6.22, s	103.6
	6.49, s		6.29, s	
N-CH_3	3.67, s	45.5	3.11, s	44.6
13-OCH_3	3.86, s	54.4	3.94, s	55.6
14-OCH_3	2.75, s	54.4	3.26, s	54.8
1′		122.4		124.1
1a'		117.8		118.0
2′		149.7		149.8
3′		160.5		160.6
4′	7.89, s	106.8	7.86, s	106.8
4a'		135.6		135.7
5′	8.42, d (6.6)	123.9	8.40, d (6.6)	123.9
6′	8.84, d (6.6)	135.7	8.80, d (6.6)	135.8
8′	5.88, d (13.8)	53.6	5.83, d (13.8)	53.3
	6.57, d (13.8)		6.49, d (13.8)	
8a'		130.5		130.1
9′		146.1		146.1
10′		155.9		156.1
11′	6.98, d (9.0)	114.1	7.10, d (8.4)	114.2
12′	6.60, d (9.0)	125.1	7.16, d (8.4)	124.6
12a'		126.8		124.7
13′		132.9		132.3
13a'		145.5		145.1
2′-OCH_3	4.06, s	61.2	4.03, s	61.2
3′-OCH_3	4.14, s	57.2	4.13, s	57.2
9′-OCH_3	4.08, s	62.0	4.05, s	62.0
10′-OCH_3	3.86, s	56.3	3.90, s	56.4

[a] Data were recorded at 600 MHz.
[b] Data were recorded at 150 MHz. The assignments were based on DEPT ^{1}H-^{1}H COSY, HSQC, and HMBC experiments.

This deduction was further confirmed by the NOESY cross-peaks of MeO-10′/H-11′, MeO-3′/H-4′, H-6′/H_2-8′, and H-4′/H-5′ (Fig. 3).

A final step to connect part **A** and part **B** was resolved by the solid HMBC correlations from H-12′ to C-9 and from H-12 to C-1′, C-2′, and C-9, thereby constructing an unprecedented 6/7/6/6/6/6 hexacyclic system in **1**. Reasuringly, this fusion was fully consistent with the NOESY correlations of H-1/H-15, H-1/H-8′a, and *N*-Me/H-12′. Also, a 1D NOE difference experiment with **1** showed enhancements of MeO-14 and H-1 when H-15 was irradiated. These observations allowed the *N*-methyl-1,6-methylenedioxyisoquinoline moiety to be perpendicularly 'inserted' below the 6/7/6/6/6/6 hexacyclic system with steric hindrance at the C-8–C-9 axis (Fig. 3), which strikingly resulted in the close spatial proximity of H-1 with H-15 and H-8′a, and *N*-Me with H-12′. At this point, it was rational to explain the extraordinary up-field shifts of MeO-14 (δ_H 2.75), H-15 (δ_H 6.29), and H-12′ (δ_H 6.60) induced by the anisotropic shielding of the *N*-methyl-1,6-methylenedioxyisoquinoline moiety (Fig. 3).

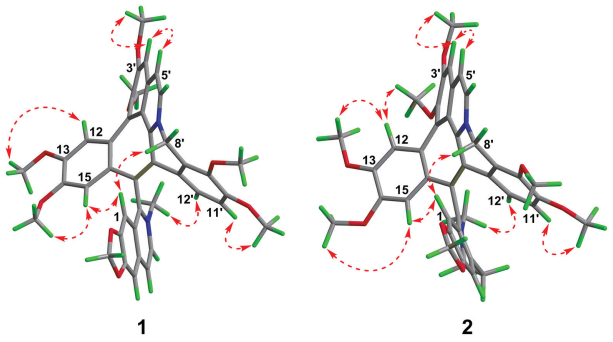

Fig. 3. Key NOESY correlations (red double arrows) for **1** and **2**.

Yanhusuosine B (**2**), also isolated as red and amorphous powder, was determined to be an alkaloid with a molecular formula of $C_{41}H_{38}N_2O_8$ based on the double-charged molecular ion at *m/z* 343.1309 (calcd. for $C_{41}H_{38}N_2O_8$, 343.1309), which differed from **1** by $+H_2$. It was clear that **2** was assigned as the $\Delta^{5,6}$ reductive analogue of **1** because the NMR signals for the double bond at C-5–C-6 in **1** were lost and replaced by two methylenes coupling to each other. The ultimate structure of **2** was completed as shown in Fig. 1 by interpretation of its 2D NMR data, especially, analogous NOESY correlations for **1** were also observed in the NOESY spectrum of **2** (Figs. 2 and 3).

With the gross structure of the novel benzylisoquinoline-protoberberine homodimers (**1**) and (**2**) established, defining the absolute axial configuration induced by the C-8–C-9 biaryl axis was proved to be more challenging owing to their lacks of [α] values and ECD Cotton effects (Figs. S14 and S26 in Supporting information). It has been reported that the rotational energy is higher than 23.3 kcal/mol that enables the atropisomers exist

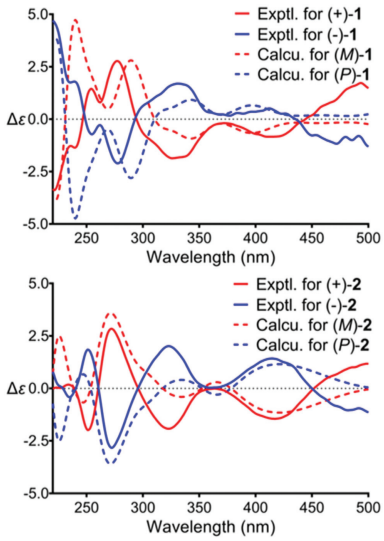

Fig. 4. Experimental and computational ECD spectra for **1** and **2**.

[23–25]. Thus, density functional theory (DFT) calculations were conducted to obtain axial conformers of **1** and **2** with rotational energy around 70 kcal/mol (Figs. S29 and S30 in Supporting information), strongly supporting the occurrence of atropisomeric mixtures of **1** and **2**. Efforts to crystallize **1** and **2** proved unsuccessful. Fortunately, **1** and **2** were separated into their pure *atropo*-enantiomers by the CHIRAL MD(2) column (Figs. S13 and S25 in Supporting information), respectively. As expected, the *atropo*-enantiomers showed fully opposite [α] values and mirror-like ECD curves each other (Fig. 4). These findings clearly demonstrated that (+)/(−)-**1** and **2** are configurationally fixed at ambient temperature

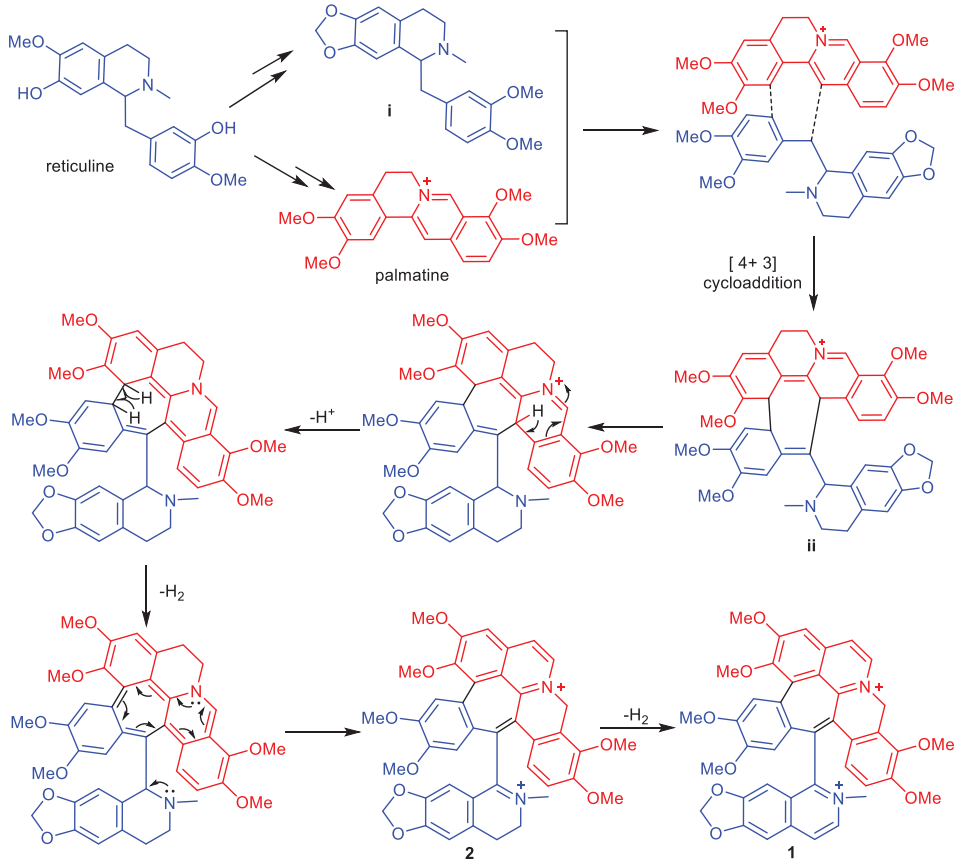

Scheme 1. Hypothetical biosynthetic pathways for **1** and **2**.

due to the highest steric congestion. Finally, the axial chirality of (+)/(−)-**1** and **2** was determined by comparing their actual electronic circular dichroism (ECD) with those predicted using time-dependent density functional theory (TDDFT) calculations.

The theoretical ECD spectra for both atropisomeric forms for **1** and **2** were in good accordance with their experimental ECD spectra (Fig. 4), which allowed the absolute axial configuration for (+)-**1**/**2** and (−)-**1**/**2** to be established as (*M*)- and (*P*)-configured, respectively. (+)-**1**/**2** and (−)-**1**/**2** were obtained as trifluoroacetate (TFA) salts due to the application of TFA during the HPLC purification.

Natural products with C−C bond-induced axial chirality have been continuously discovered during the recent decades, but rare in BBIAs [24,26]. The unusual 6/7/6/6/6/6 hexacyclic system coupled with an isoquinoline moiety *via* a C−C bond present in **1** and **2** has never been described in natural products chemistry. A retro-assembly analysis proposed that **1** and **2** probably biosynthesized from a molecule of benzylisoquinoline with a unit of protoberberine *via* an intermolecular [4+3] cycloaddition which contributed directly to seven-membered rings common in natural products [27]. Plausible biosynthetic origin of **1** and **2** were proposed in Scheme 1 with reticuline served as the upstream precursor, a very important intermediate to biosynthesize all types of bioactive BIAs including palmatine, morphine, berberine, *etc*. [14,28]. Briefly, reticuline would be transformed into intermediate **i**, which undergo an intermolecular [4 + 3] cycloaddition with palmatine to form a key intermediate **ii** with 6/7/6/6/6/6 hexacyclic system. Subsequently, the intermediate **ii** is converted to **2** and **1** through sequences of deprotonation and dehydrogenation.

Our last task was to evaluate **1** and **2** for biological activities *in vitro*. The *in vitro* anti-inflammatory properties of compounds **1** and **2** were evaluated against NO production in LPS-induced RAW264.7 macrophage cells. As a result, compound **2** showed moderate inhibitory activity with the IC_{50} value of 8.24 ± 0.73 μmol/L, which is more potent than the clinically used agent indomethacin (IC_{50} = 13.43 ± 4.06 μmol/L). In addition, the cytotoxic activity of **1** and **2** were evaluated in human breast cancer cells (MCF-7), human hepatoma cells (HepG2), and human ovarian cancer cells (HO-8910) by the thiazolyl blue bromide (MTT) assay. However, no cytotoxicity was found for both compounds **1** and **2** at 50 μmol/L in the above cell lines.

In summary, as a new class of alkaloid dimers with an unprecedented 6/7/6/6/6/6 hexacyclic skeleton, (+)/(−)-yanhusuosines A (**1**) and B (**2**) would attract much attention from both chemists and biologists, and further studies such as synthesis and in-depth biological tests are warranted.

Declaration of competing interest

The authors declare that they have no known competing financial interests or personal relationships that could have appeared to influence the work reported in this paper.

Acknowledgments

This study was supported by the National Natural Science Foundation of China (No. 82073978), the Fundamental Research Funds for the Central Universities (No. 2022-JYB-JBZR-015) and Beijing Natural Science Foundation (No. JQ18026).

Supplementary materials

Supplementary material associated with this article can be found, in the online version, at doi:10.1016/j.cclet.2022.108073.

References

[1] H. Guinaudeau, A.J. Freyer, M. Shamma, Nat. Prod. Rep. 3 (1986) 477–488.
[2] P.L. Schiff, J. Nat. Prod. 50 (1987) 529–599.
[3] P.L. Schiff, J. Nat. Prod. 54 (1991) 645–749.
[4] P.L. Schiff, J. Nat. Prod. 60 (1997) 934–953.
[5] V.K. Nguyen, K.G.M. Kou, Org. Biomol. Chem. 19 (2021) 7535–7543.
[6] C. Weber, T. Opatz, Alkaloids Chem. Biol. 81 (2019) 1–114.
[7] J.Q. Qian, Acta Pharmacol. Sin. 23 (2002) 1086–1092.
[8] I. Galindo, U. Garaigorta, F. Lasala, et al., Antiviral Res. 186 (2021) 104990.
[9] S. Zhang, W. Huang, L. Ren, et al., Cell Res. 32 (2022) 9–23.
[10] L.Y. Wang, B.L. Qiu, H. Xia, et al., J. Nat. Prod. 83 (2020) 489–496.
[11] L. Alhassen, T. Dabbous, A. Ha, et al., Molecules 26 (2021) 7498.
[12] B. Tian, M. Tian, S.M. Huang, Pharm. Biol. 58 (2020) 265–275.
[13] J. Zhang, S. He, J. Wang, et al., Nat. Prod. Commun. 15 (2020) 1–19.
[14] D. Xu, H. Lin, Y. Tang, et al., Hortic. Res. 8 (2021) 16.
[15] N. Cabedo, I. Berenguer, B. Figadere, et al., Curr. Med. Chem. 16 (2009) 2441–2467.
[16] C.M. Sai, D.H. Li, C.M. Xue, et al., Org. Lett. 17 (2015) 4102–4105.
[17] G.Y. Xia, B.B. Xiao, L.Y. Wang, et al., Acta Pharm. Sin. 56 (2021) 553–556.
[18] B.B. Xiao, G.Y. Xia, L.Y. Wang, et al., Tetrahedron Lett. 61 (2020) 151890.
[19] S. Fayez, J. Li, D. Feineis, et al., J. Nat. Prod. 82 (2019) 3033–3046.
[20] B.K. Lombe, T. Bruhn, D. Feineis, et al., Org. Lett. 19 (2017) 1342–1345.
[21] B.K. Lombe, T. Bruhn, D. Feineis, et al., Org. Lett. 19 (2017) 6740–6743.
[22] M. Xu, T. Bruhn, B. Hertlein, et al., Chemistry 16 (2010) 4206–4216.
[23] G.J. Mei, W.L. Koay, C.Y. Guan, et al., Chem 8 (2022) 1855–1893.
[24] J.E. Smyth, N.M. Butler, P.A. Keller, Nat. Prod. Rep. 32 (2015) 1562–1583.
[25] X.L. Min, X.L. Zhang, R. Shen, et al., Org. Chem. Front. 9 (2022) 2280–2292.
[26] B.K. Lombe, D. Feineis, G. Bringmann, Nat. Prod. Rep. 36 (2019) 1513–1545.
[27] Z. Yin, Y. He, P. Chiu, Chem. Soc. Rev. 47 (2018) 8881–8924.
[28] Z. Xu, Z. Li, F. Ren, et al., Plant J. 111 (2022) 217–230.